

Pulsed Laser Induced Deformation in an Fe-3 Wt Pct Si Alloy

A. H. CLAUER, B. P. FAIRAND, AND B. A. WILCOX

The plastic deformation produced by laser induced stress waves was investigated on an Fe-3 wt pct Si alloy. The intensity and duration of the stress waves were varied by changing the intensity and pulse length of the high energy pulsed laser beam, and also by using different overlays on the surfaces of the specimens. The resulting differences in the distribution and intensity of the deformation caused by the stress waves within the samples were determined by sectioning the specimens and etching (etch pitting) the transverse sections. The magnitude of the laser shock induced deformation depended on the laser beam power density and the type of surface overlay. A combination transparent plus opaque overlay of fused quartz and lead generated the most plastic deformation. For both the quartz and the quartz plus lead overlays, intermediate laser power densities of about $5 \times 10^8 \text{ w/cm}^2$ caused the most deformation. The shock induced deformation became more uniform as the thickness of the material decreased, and uniform shock hardening, corresponding to about 1 pct tensile strain, was observed in the thinnest specimens (0.02 cm thick). 200 ns laser pulses caused some surface melting, which was not observed for 30 ns pulses, the pulse length used in most of the experiments. Deformation of the Fe-3 wt pct Si alloy occurred by both slip and twinning.

HIGH power pulsed lasers generate stress or shock waves in a target sample by subjecting it to very short pulses of intense laser light. The resultant disturbance in the sample is primarily mechanical since the thermal effects are small and confined to a region within a few micrometers from the laser irradiated surface.

The shock wave is created by the momentum impulse imparted to the specimen's surface when a thin surface layer is rapidly vaporized by the intense laser light. Since this process depends on effectively coupling the laser energy into the specimen's surface, the magnitude of the pressure is affected by such factors as the surface condition, its reflectivity, and the target material's sublimation and ionization energy. Also, phenomena occurring within the blowoff material which absorb, reflect, or reradiate energy, such as the formation of a plasma, limit the amount of energy reaching the surface of the specimen. For these reasons, it was anticipated that the modification of surface conditions through the use of various overlay materials, and blowoff confinement by transparent overlays would affect the peak pressures. In addition, modifications of the pulse length and shape could also influence the magnitude and length of the pressure pulse.

Various recent studies have examined methods of modifying the material surface conditions to enhance the magnitude of laser induced shock waves.¹⁻⁴ It has been shown that a 7075 aluminum alloy was shock hardened after irradiation with a high power, Q switched laser through a transparent quartz overlay covering the target specimen.⁵ Another study showed that very short ($\sim 1 \times 10^{-9}$ s), high fluence pulses could cause back surface spalling in thin aluminum discs irradiated in vacuum.⁶

This paper reports on a series of experiments which relate the magnitude and extent of shock induced plastic deformation produced in an Fe-3 wt pct Si alloy to the laser pulse length and power density for several different types of surface overlays. The overlays studied include a transparent overlay to confine the blowoff material to the sample surface and an overlay of lead, which has a low sublimation energy. The etch pit patterns on the Fe-3 pct Si specimens after shocking and sectioning are qualitatively correlated with the measured and predicted shock pressures. A previous paper⁷ presents the computer code calculations, laser physics, and pressure environments for the experiments discussed here.

EXPERIMENTAL PROCEDURES

Material

An Fe-3 wt pct Si alloy (Si: 3.63, C: 0.026, N: 0.002, and O: 0.017 wt pct) was chosen for the laser shocking studies because it can be readily etch pitted to show the distribution and approximate magnitude of plastic deformation. The starting material was prepared as described by Hahn, et al.⁸ 24 to 48 h prior to the laser shocking experiment, the specimens were solution annealed at 780°C for 4 h, air cooled, and immediately stored on ice to inhibit aging. After the laser irradiation the specimens were aged for 20 min at 150°C. This treatment caused only the dislocations present at the time of aging, including those formed during shocking, to be revealed after subsequent sectioning and etching.

Laser Shocking

The laser shocking experiments were performed with a CGE Model VD-640, Q switched neodymium glass laser which consists of an oscillator followed by five amplifier stages. This system is capable of emitting up to 500 J of laser energy in a pulse that is approximately triangular in shape, with a full width at half maximum of 25 to 30 ns. The laser radiation was focused onto the samples in spot diameters of up to 3 cm with a 100 cm focal length lens. Monitoring of the laser pulse showed the reproducibility of the laser pulse shape was very good.⁷

The Fe-3 pct Si samples were machined from as-rolled plate in the form of 1.9 cm diam. discs, and then lapped to their final thicknesses to obtain the flat, parallel surfaces required for pressure measurements. Most specimens were 0.3 cm thick, but a series of thinner specimens were prepared to study microstructure changes and pressure wave attenuation as a function of thickness.

The four surface conditions studied, shown in Fig. 1, consisted of a bare Fe-3 pct Si surface, a fused quartz overlay, a lead overlay, and a fused quartz-plus-lead overlay. In most experiments, the sample surface was covered with an overlay of fused quartz in the form of a disc 2.5 cm in diam and 0.3 cm thick, either with or without a 10 μ m thick lead foil overlay placed between the quartz and the specimen surface. The sandwich was clamped firmly against a lapped surface by a fine threaded brass cap having a 1.65 cm diam hole for entrance of the laser beam, and the quartz pressure transducer was then threaded up through a center hole in the holder and pulled finger tight against the back surface of the sample. Good coupling between the gage and sample back surface was further insured by placing a thin layer of mineral oil at this interface. In most cases the laser beam was spread to a diameter of about 1 to 2

cm. This variation in beam diameter assisted in achieving a variety of power densities.

Metallographic Studies

After shocking and aging, the samples were sectioned perpendicular to the face of the disc along a diameter through the approximate center of the laser spot. Transverse faces of the specimens were metallographically ground and then electrolytically polished and etched 10 min in the Morris' solution to reveal the shock induced dislocations as etch pits.⁸ Micrograph montages were made of the relevant part of the cross section at 50 to 100 times magnification to show the shock deformation pattern.

RESULTS AND DISCUSSION

Influence of Surface Condition and Overlays

Initially, the effect of different surface conditions was investigated for a range of power densities and a laser pulse approximately 30 ns long at half maximum. Table I gives the salient experimental conditions and measured backface peak pressures. Samples having bare surfaces (Fig.1(a)) were irradiated at power densities from 5.23×10^8 to 1.58×10^9 w/cm². The resultant deformation was very light and was confined to within 50 μ m of the surface at the highest power density, as shown in Fig. 2. The depth of deformation was lower at the lower power densities. The light etching layer near the specimen surface underwent fairly extensive plastic flow. Using the etch pitting results of Hahn, et al ⁸ as a rough calibration, this region was deformed an amount equivalent to, or greater than, ~7 pct tensile strain. The strain gradient decreased sharply with distance from the surface, and the dark etching region at a depth of ~25 to 30 μ m would be equivalent to about 0.5 to 1 pct tensile strain.

An overlay of lead, which has a low sublimation energy, was pressed against the Fe-3 pct Si sample surface (Fig. 1(b)), and irradiations at power densities of 1.08×10^9 and 2.30×10^9 w/cm² were made. The shock induced deformation was confined to a narrower surface layer than shown in Fig. 2 and was less intense. This is possibly because the lead overlay thickness was a significant fraction of the depth of the damaged layer. Pressure measurements were not made in this series of experiments.

Fe-3 pct Si samples covered by a transparent overlay only (Fig.1(c)) were irradiated at power densities of 7.11×10^8 to 3.89×10^9 w/cm². The shock deformation at increasing power densities is shown in Fig. 3. Duplicate experiments were run in each case with similar results. The intensity and extent of the shock deformation was largest at a power density of about 1×10^9 w/cm². The heaviest deformation occurred in the central region of the disc near both the front and back surfaces for the higher power densities, but only at the front surface at the lower power densities.

Samples having combined transparent and lead overlays (Fig.1(d)) were irradiated at power densities of 2.78×10^8 to 4.04×10^9 w/cm². The etched cross sections of discs laser shocked at increasing power densities are shown in Fig. 4. Under these conditions a laser power density of about 5×10^8 w/cm² most effectively coupled laser energy into the sample.

The lead overlay was selected because it has a lower sublimation energy than iron. Thus for a given energy density, more lead would be vaporized than iron, giving a larger momentum impulse and thereby a higher pressure. A higher front face pressure for the quartz plus lead overlay is implied by comparing Fig. 4(b) with Fig. 3(a). However, a comparison of Fig. 3(c) and 4(c) shows that at a higher power density, the pressure enhancement by the lead overlay is lost. This is possibly because the ionization characteristics of the lead lowers the threshold for plasma formation in the blowoff gas. The plasma reflects most of the laser energy away from the specimen surface and this would substantially reduce the amplitude or length of the stress wave.

It was expected that the deformation revealed by etch pitting would be heaviest at the front surface, tapering off to the back surface since pressure wave attenuation measurements showed that the shock wave attenuated rapidly with distance from the front surface.⁷ Although the front surface pressure was about 56 kbar, the peak pressure was down to about 10 kbar within about 0.15 cm travel from the front surface. The back surface pressure measurements presented in Table I show that in most cases, the pressure dropped only slightly below 10 kbar in the remaining 0.15 cm to the back surface. The absence of heavy deformation in the region on the horizontal center line of the cross sections shown in Fig. 3(b) and (c), and to some extent, Fig. 4(b), indicate that 10 kbar is insufficient to cause significant plastic deformation.

The observed shock deformation patterns thus result from the complex, multiple interactions of the longitudinal waves with the radial release waves which propagated in from the circumferences of the discs. That this happens in experiments where guard rings and momentum traps are not used has been recognized for some time. Stevens and Jones¹⁰ demonstrated, for aluminum alloys, the complexity of the wave interactions using computer calculations for discs of similar size and shape to the Fe-3 pct Si discs. Although the shock conditions they used were different from the laser shocks obtained here, the overall effects may be similar, particularly because after the decay of the narrow, high pressure pulse, the low level pressure pulse is several hundred nanoseconds long. Their results showed that the radial release waves focused on the axis of the disc and increased the local tensile stress sufficiently to generate additional plastic flow at that point (Fig. 4(b)). It is suggested that the symmetrical deformation patterns in the upper and lower halves of the specimens in Figs. 3(b) and 4(b) is also caused by the multiple interactions of the longitudinal and radial wave systems as they reverberate through the specimen. The amplitude of the longitudinal waves will be less than the back face pressure and the radial waves will also be of a low level, but the superposition and focusing effects would create local peaks in stress above the elastic limit and would thus induce plastic flow. In general terms, the intensity of the observed plastic deformation is still related to the magnitude and length of the pressure pulse produced by the laser light.

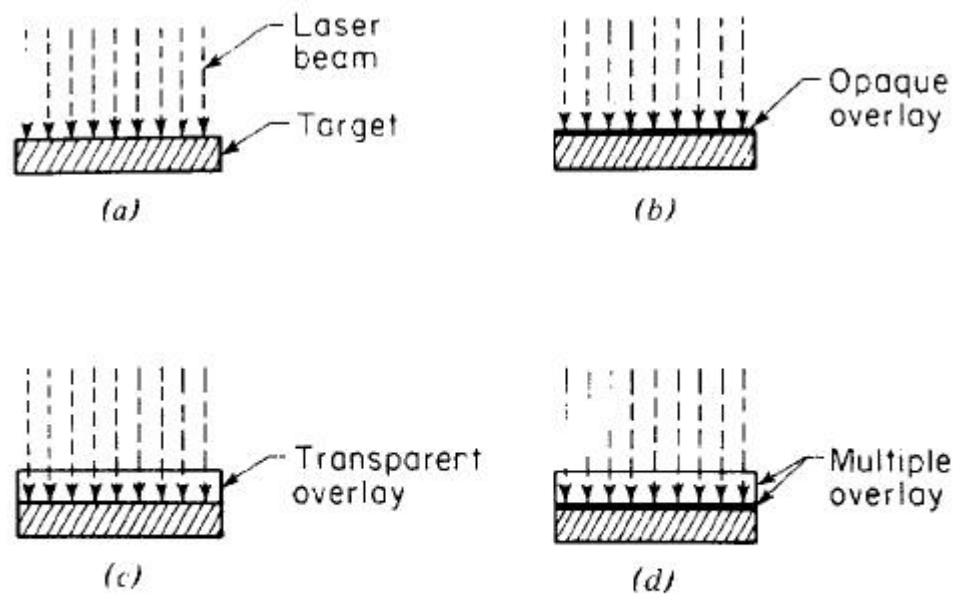


Fig. 1—Overlay configurations used in this study. (a) Bare Fe-3 pct Si disc; (b) Pb overlay; (c) fused quartz overlay; and (d) fused quartz plus lead overlay.

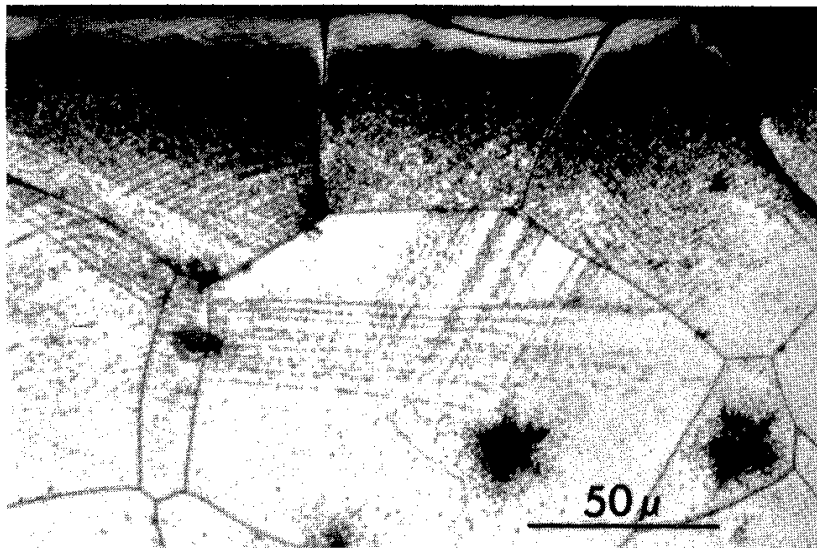


Fig. 2—Deformation damage after irradiating the bare surface at 1.58×10^9 w/cm². The top surface was irradiated.

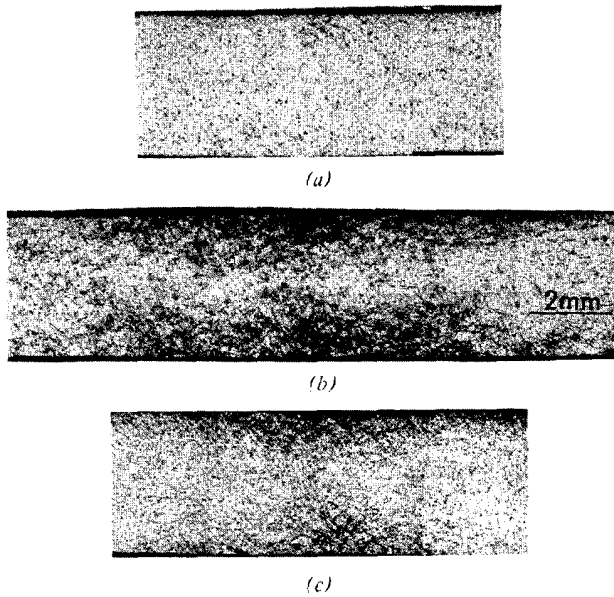


Fig. 3—Montages from central regions of sections of 0.3 cm thick discs after laser shocking over a range of power densities. The top surfaces of the specimens were covered with a fused quartz overlay. (a) Irradiated at 7.11×10^8 w/cm² with a 1.27 cm spot diameter; (b) irradiated at 1.08×10^9 w/cm² with a 1.9 cm spot diameter; (c) irradiated at 3.89×10^9 w/cm² with a 0.65 cm spot diameter.

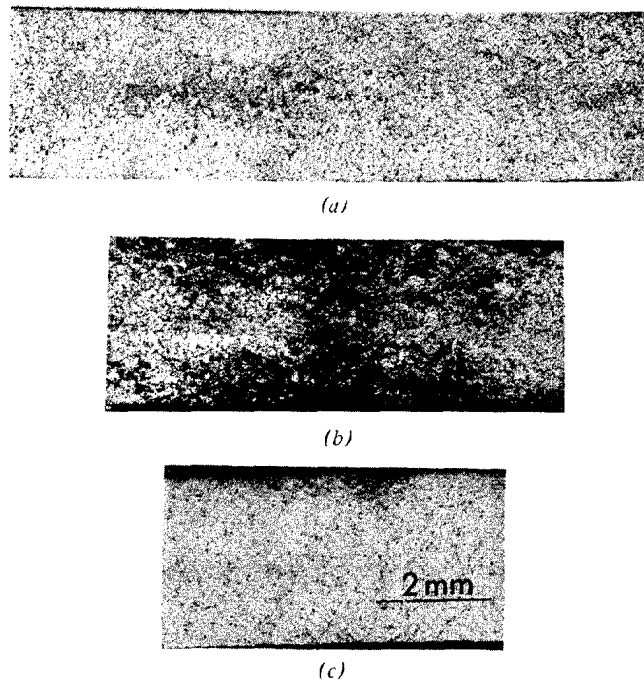


Fig. 4—Montages from central regions of sections of 0.3 cm thick discs after laser shocking over a range of power densities. The top surfaces of the specimens were covered with fused quartz-plus-lead overlays. (a) Irradiated at 2.78×10^8 w/cm² with a 2.7 cm spot diameter; (b) irradiated at 5.54×10^8 w/cm² with a 2.7 cm spot diameter; (c) irradiated at 4.04×10^9 w/cm² with a 0.65 cm spot diameter.

Table I. Summary of the Laser Irradiated Samples for Both Metallographic Examination and Pressure Measurements

Sample Number*	Thickness, mm	Back Face Pressure, kbar	Overlay Configuration	Pulse Length, ns	Power Density, w/cm ²	Energy Density, J/cm ²	Spot Diameter, cm
Influence of Surface Conditions and Overlays							
1	3.053	—	Bare	30	5.23×10^8	15.6	2.7
2	3.053	0.4	Bare	35	8.85×10^8	30.9	2.7
3	3.053	—	Bare	40	1.51×10^9	60.6	1.9
4	3.053	—	Bare	40	1.58×10^9	63.1	1.6
5	3.035	—	Lead	30	1.08×10^9	32.3	2.7
6	3.053	—	Lead	40	2.30×10^9	92.0	1.6
7	3.002	9.2	Quartz	25 to 30	7.11×10^8	17.8	2.5
8	2.992	—	Quartz	35	8.0×10^8	28.0	2.7
9	3.023	—	Quartz	40	1.08×10^9	43.3	1.9
10	3.035	—	Quartz	30	1.10×10^9	32.9	2.7
11	3.035	8.2	Quartz	30	3.35×10^9	100.5	1.6
12	3.002	8.6	Quartz	25 to 30	3.89×10^9	97.2	1.3
13	3.035	9.1	Quartz and lead	70	2.78×10^8	19.5	2.7
14	2.997	9.9	Quartz and lead	40	5.5×10^8	21.7	2.7
15	3.023	—	Quartz and lead	30	5.64×10^8	16.9	2.7
16	3.002	9.4	Quartz and lead	25 to 30	9.34×10^8	24.6	2.5
17	3.045	6.5	Quartz and lead	30	3.02×10^9	90.5	1.6
18	2.997	8.2	Quartz and lead	25 to 30	4.04×10^9	101.0	1.3
Influence of Specimen Thickness							
19	0.014 [†]	56.6	Quartz	25 to 30	1.25×10^9	31.2	2.5
7	3.002	9.2	Quartz	25 to 30	7.11×10^8	17.8	2.5
12	3.002	8.6	Quartz	25 to 30	3.89×10^9	97.2	1.3
9	3.023	—	Quartz	40	1.08×10^9	43.3	1.9
20	1.808	—	Quartz	25 to 30	1.22×10^9	30.6	2.5
21	1.808	8.8	Quartz	25 to 30	1.15×10^9	28.8	2.5
22	0.927	18.0	Quartz	25 to 30	1.24×10^9	31.0	2.5
23	0.516	—	Quartz	25 to 30	1.0×10^9	25.0	2.5
24	0.523	—	Quartz	25 to 30	1.03×10^9	25.8	2.5
25	0.157	—	Quartz	25 to 30	1.31×10^9	32.7	2.5
Influence of Pulse Length							
7	3.002	9.2	Quartz	25 to 30	7.11×10^8	17.8	2.5
12	3.002	8.6	Quartz	25 to 30	3.89×10^9	97.2	1.3
26	3.048	9.6	Quartz	200	1.1×10^9	224.0	0.8
27	3.048	7.1	Quartz	200	4.5×10^8	90.1	0.8

*Some of the samples are repeated in the different sections of the table to facilitate comparisons.

[†]Iron film deposited on 3-mm thick quartz disc.

Influence of Specimen Thickness

The effect of decreasing sample thickness was studied at a power density of nominally 1.0×10^9 w/cm^2 with a fused quartz overlay, and the results are given in Table I and Fig. 5. As shown in Fig. 5, the amount of deformation at the front and back surfaces was about the same with decreasing thickness, but the lightly deformed central layer increased in width with increasing specimen thickness. The thinner specimens were heavily deformed over most of the thickness. Significant hardening through the disc thickness, equivalent to about 1 pct tensile strain, was observed in the 0.02 cm thick disc. Hardness measurements at the center of the section shown in Fig. 5(d) gave Knoop hardness numbers ranging from 260 to 320 compared with hardnesses of 210 to 240 for unshocked material and at the center of the specimen in Fig.5(a). Thus, in thin sections, significant hardening throughout the material can be achieved by pulsed laser radiation.

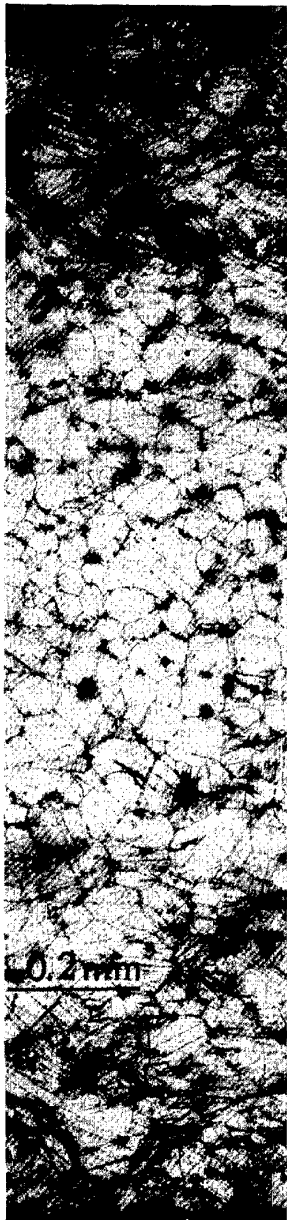
Influence of Pulse Length

The effects of laser pulses 200 ns long, using a quartz overlay, were studied at power densities of 1.45×10^8 w/cm^2 and 1.12×10^9 w/cm^2 . Fig. 6 shows the shape of the stress wave at the back surface for a long and short pulse. The back surface peak pressure was the same for the long and short pulses, but the long pulse pressure was still high after 500 ns, the length of the observation period, whereas the shock wave pressure of the short pulse decreased much more rapidly. This may be the reason for the deformation appearing to be more uniformly distributed in the sample irradiated by a long pulse, shown in Fig. 7, although the magnitude of the deformation is small. The microstructure was similar to that shown in Fig. 7 for both power densities used.

The long laser pulses did cause some surface melting as shown in Fig. 8. Although some surface roughening occurred at the lower pulse times, no melting was observed. It is expected that a heat affected zone will extend deeper into the specimen for long pulses than for short ones. A crude estimate of the depth of the thermal front reached during the 200 ns laser pulse is given by $x = 2\sqrt{kt}$, where x is the depth reached, k is the thermal diffusivity, and t is the pulse length. Using, for iron, $k = 0.18$ cm^2/s , and $t = 200$ ns, $x = 3.8$ μm . This heat will dissipate rapidly after the pulse ends; thus, the severely heat affected layer probably extends less than 10 μm in from the surface. The distance for the shorter 30 ns pulse is less than half of that.

DEFORMATION MECHANISMS

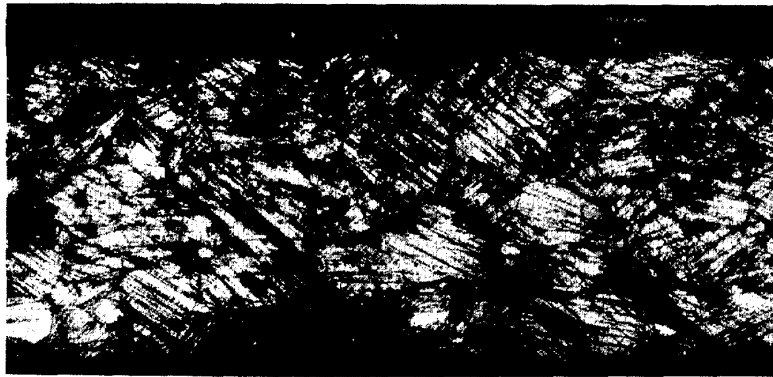
The deformation in shocked samples is primarily slip (Figs. 2 and 9(a)), but twinning is also observed (Fig. 9(b)). The twins are long and very narrow, and generate local slip where they intersect as well as between neighboring parallel twins, marked A and B, respectively, in Fig.9(b). Taylor has shown that twins are generated at pressures just above the Hugoniot Elastic Limit (The Hugoniot Elastic Limit is the maximum pressure a crystal will support before yielding in shear. See Ref. 9) in iron¹¹, but whether slip or twinning occurs will depend upon the magnitude and duration of the shock pressure and possibly on the stress rate of the rarefaction wave. The extent of slip will also depend on these factors.



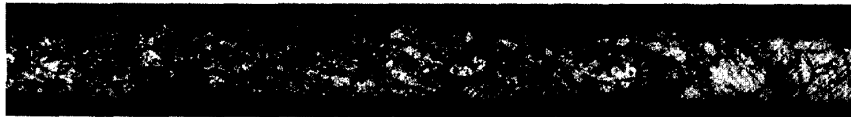
(a)



(b)



(c)



(d)

Fig. 5—Shock deformation as a function of sample thickness. The top surfaces were covered with a fused quartz overlay. ϕ is the power density used, t is the specimen thickness, and P is the measured backface pressure. (a) $t = 0.181$ cm, $\phi = 1.15 \times 10^9$ w/cm², $P = 5.8$ kbar; (b) $t = 0.093$ cm, $\phi = 1.24 \times 10^9$ w/cm², $P = 18$ kbar; (c) $t = 0.051$ cm, $\phi = 1.03 \times 10^9$ w/cm², P , not measured; (d) $t = 0.020$ cm, $\phi = 1.31 \times 10^9$ w/cm², P , not measured.

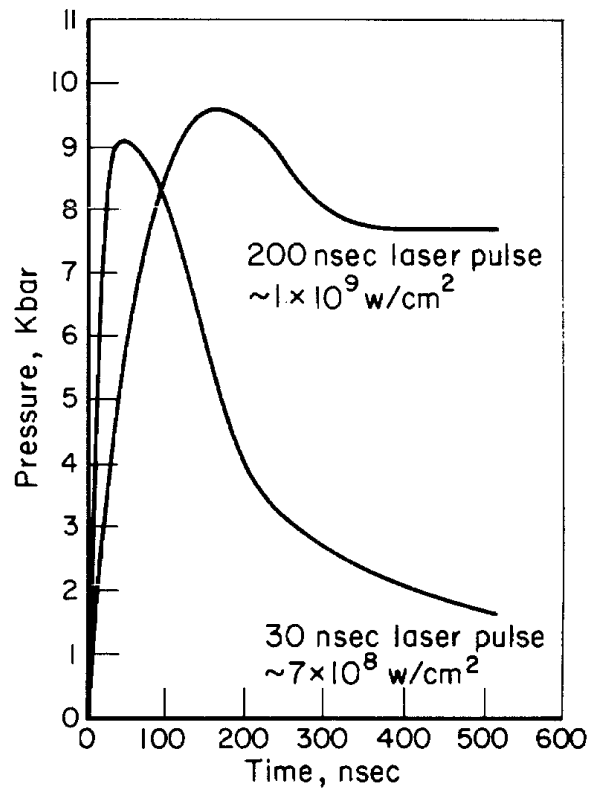


Fig. 6—Comparison of the shape of the stress wave at the back face for long and short laser pulses. Fused quartz overlay.

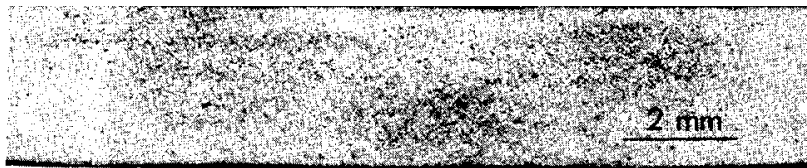


Fig. 7—Cross section of the 0.3 cm thick sample irradiated with a 200 ns laser pulse at 1.12×10^9 w/cm² and a beam diameter of 0.8 cm. The top surface was covered with a fused quartz overlay.

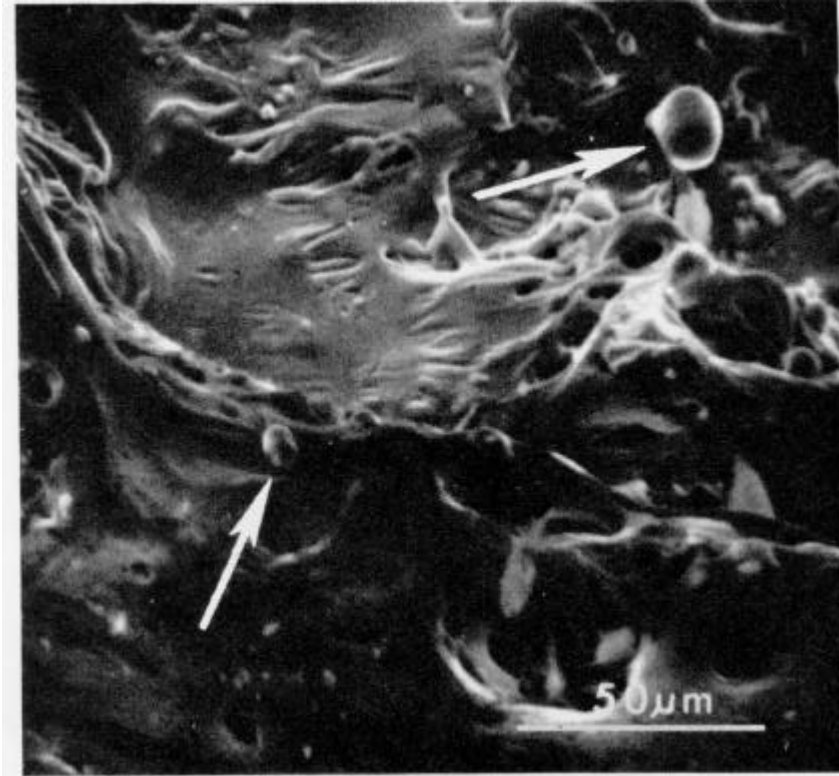
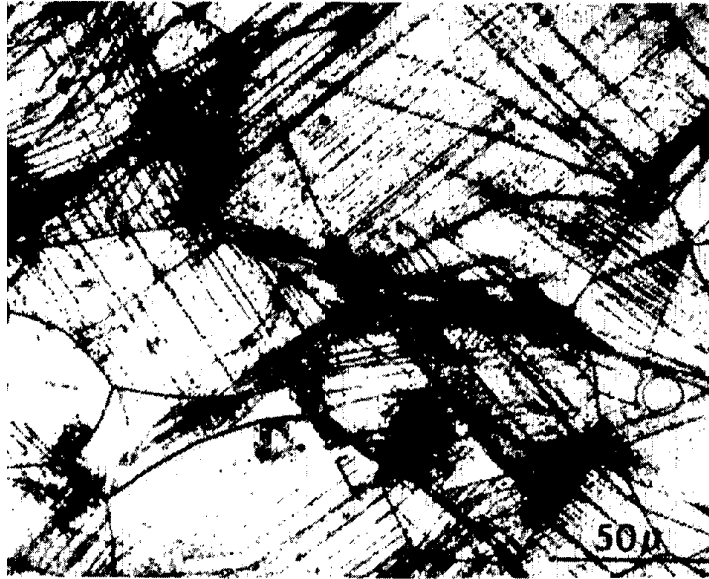
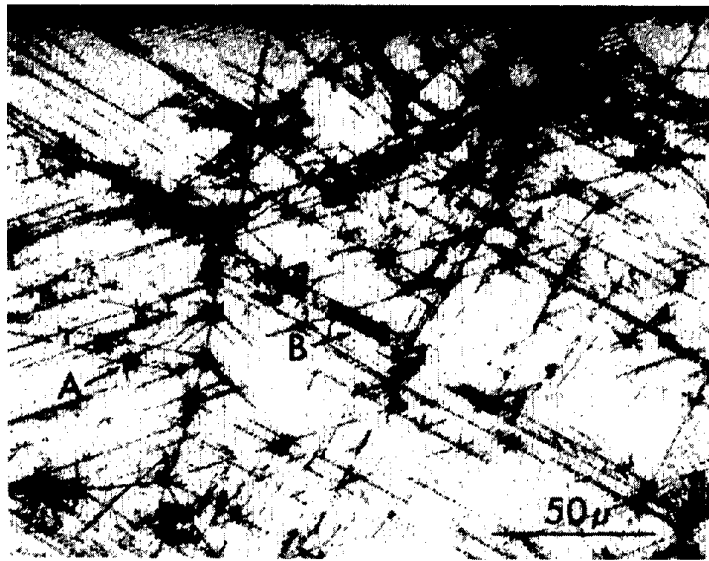


Fig. 8—Scanning electron micrograph of the surface of the Fe-3 pct Si specimen exposed to a 200 ns laser pulse. Arrows indicate resolidified droplets.



(a)



(b)

Fig. 9—Slip and twinning present in areas away from the heavily deformed regions. (a) Representative slip line pattern in sample shown in Fig. 3(c); (b) narrow twins in sample shown in Fig. 4(b).

CONCLUSIONS

- 1) Pressures sufficient to cause extensive plastic flow in an Fe-3 wt pct Si alloy have been generated by irradiating specimens covered by surface overlays with a high power pulsed laser. Deformation occurs by both slip and twinning.
- 2) Studies of various surface conditions (bare surface, transparent quartz overlay, lead foil overlay, and quartz-plus-lead overlay) showed that the quartz-plus-lead overlays produced the most deformation for a given laser power density. The quartz acts to confine the vaporized metal, and the lead, which has a lower sublimation energy than iron, vaporizes readily.
- 3) Irradiation of specimens of varying thickness showed that uniform deformation, corresponding to about 1 pct tensile strain, could be produced in 0.02 cm thick specimens. For thicker specimens, the central regions were less heavily deformed than the surfaces.
- 4) The magnitude of the deformation increased with increasing laser power density with the quartz overlay, but decreased at the higher power densities with the quartz-plus-lead overlay.
- 5) Several specimens irradiated with 200 ns pulses showed some surface melting (not observed after the shorter pulses), but no increase in the measured back surface peak pressure relative to specimens irradiated with 30 ns pulses.

ACKNOWLEDGMENT

We are grateful for the support of this research by the Division of Materials Research, National Science Foundation, under Grant DMR-72-03277.

REFERENCES

1. M. Siegrist and F. K. Kneubuhl: *Appl. Phys.*, 1973, vol. 2, pp. 43-44.
2. J. D. O'Keefe and C. H. Skeen: *J. Appl. Phys.*, 1973, vol. 44, pp. 4622-26.
3. Jay A. Fox: *Appl. Phys. Lett.*, 1974, vol. 24, pp. 461-64.
4. L. C. Yang: *J. Appl. Phys.*, 1974, vol. 45 pp. 2601-08
5. B. P. Fairand, B. A. Wilcox, W. J. Gallagher, and D. N. Williams: *J. Appl. Phys.*, 1972, vol. 43, pp. 3893-95.
6. J. A. Fox and D. N. Barr: *Appl. Phys. Lett.* 1973, vol. 22, no. 11 pp. 594-96.
7. B. P. Fairand, A. H. Clauer, R. G. Jung, and B. A. Wilcox: *Appl. Phys. Lett.*, 1974, vol. 25, pp. 431-33.
8. G. T. Hahn, P. N. Mincer, and A. R. Rosenfield: *Exp. Mech.*, 1971, vol. 11, pp. 248-54.
9. G. E. Duvall and G. R. Fowles: *High Pressure Physics and Chemistry*, R. S. Bradley, ed., vol. 2, p. 271, Academic Press, New York, 1963.

10. A. L. Stevens and O. E. Jones: *J. Appl. Mech.*, 1972, vol. 39, pp. 359-66.
11. J. W. Taylor: referenced by E.G. Zukas, C. M. Fowler, F. S. Minshall, and J. O'Rourke, *Trans. TMS-AIME*, 1963, vol. 227, pp. 746-53.